Analyses of drift stability and rockfall due to earthquake ground motion at Yucca Mountain, Nevada

Rui Chen
Center for Nuclear Waste Regulatory Analyses, Southwest Research Institute, US

ABSTRACT: A technical issue of concern in the performance assessment of the proposed repository at Yucca Mountain (YM) is potential damage to the waste packages (WPs) emplaced in the drifts by direct rockfall due to earthquake ground motion. This is of particular interest because the rock mass surrounding the proposed repository is highly fractured and YM is located in a seismically active region. This paper analyzes rockfall phenomena by simulating the behavior of an unsupported emplacement drift undergoing repeated seismic ground motion after subjecting it to *in situ* stress and, for some cases, a time-decaying thermal load generated by the emplaced wastes. Preliminary modeling results show that fracture pattern and block size have a controlling effect on the number of blocks falling simultaneously, the extent of rockfall, and the overall drift stability. Other factors that may affect rockfall are also discussed, including characteristics of seismic ground motion, model setup, and rock and fracture thermal-mechanical properties.

1 INTRODUCTION

The proposed geological repository for high-level waste (HLW) at Yucca Mountain (YM), Nevada, is located in the tectonically active central Basin and Range Province of the North American Cordillera (Wernicke 1992). Numerous Quaternary faults, volcanoes, paleoearthquakes, and historic earthquakes are evidence of the tectonic activity of the region. Recent seismic hazard analyses (Wong & Stepp 1998) show that the mean horizontal peak ground acceleration at the reference rock outcrop (at the repository depth without over burden rock) is about 0.55 g and 1.32 g for 10,000-yr and 100,000-yr return period earthquakes, respectively. Such earthquakes may affect the integrity and radiological safety of the proposed repository because of possible disruptions to underground openings, particularly because the rock mass surrounding the proposed repository is highly fractured and contains irregular fracture patterns (Brechtel et al. 1995, Lin et al. 1993, Anna 1998). Potential damage to the waste packages (WPs) emplaced in the drifts by direct rockfall due to earthquake ground motion needs to be considered in repository performance assessment. This paper studies such rockfall, including assessing the size of rock blocks that can fall, the possibility of multiple rock blocks falling simultaneously, the extent of the potential rockfall region, and the overall stability of an emplacement drift.

9903080076 990122
PDR WASTE

Size of individual rock blocks that can fall is controlled by geometrical characteristics of the fracture network, including fracture spacing, orientation, persistence, and trace length. The primary fracture sets based on stereographic projections (Pye et al. 1997) of fracture data from the detailed line survey in the exploratory studies facility (ESF) drifts were used to generate irregular fracture patterns for use in this study. Rockfall phenomena were then analyzed with a drift scale model consisting of a single emplacement drift using the distinct element computer code UDEC (Itasca Consulting Group, Inc. 1996). The UDEC analyses simulated the behavior of an unsupported emplacement drift undergoing repeated earthquake ground motion after subjecting it to *in situ* stress and, for some cases, time-decaying thermal load generated by the emplaced wastes. In the cases with thermal loading, thermal analyses were conducted for the first 100 yr following waste emplacement, corresponding to the preclosure period. Seismic load was, then, applied to simulate rockfall during the early postclosure period (after 100 yr). Rockfall due to seismic load is not considered to affect the WPs during the preclosure period, because ground support systems will be in place during the preclosure period to protect WPs from rockfall. It can be considered that the thermal-mechanical (TM) analyses of this study apply to the preclosure period and the dynamic analyses apply to the early postclosure period. The cooling phase is not simulated and will be studied in the future.

2 MODEL DESCRIPTION

2.1 *Input parameters*

Important input to the dynamic analyses includes fracture pattern, ground motion time histories, thermal loading, and rock block and fracture TM properties. These input parameters were selected based mainly on the U.S. Department of Energy (DOE) site characterization data and repository design considerations as detailed in the following paragraphs.

Abundant information on fracture characteristics at YM has been collected by the DOE through site characterization activities, including core hole exploration (Brechtel et al. 1995, Lin et al. 1993), surface mapping, and full-periphery geological mapping and detailed line survey in the ESF (Beason 1997, Anna 1998). Detailed analyses of these fracture data are still in progress. For the current study, analyses of fracture orientations, frequencies, and fracture sets for the TSw2 (the host formation of the proposed repository), based on the detailed line survey data along the ESF main drift, were used as the basis to generate fracture patterns for dynamic analyses (Pye et al. 1997).

Using stereographic projections (Schmidt equal area lower hemisphere projection), three primary fracture sets were identified (Pye et al. 1997) with fracture spacings following log-normal distributions. The UDEC command JSET was used to generate an approximation of these three fracture sets (Table 1). Three cases were analyzed. Case A considered two primary fracture sets and, consequently, has larger size blocks. Cases B and C had three fracture sets. Block size around the opening in case C is slightly smaller than that in case B in an attempt to evaluate the effect of block size on rockfall. The purpose of selecting three cases for the current analyses was to broadly examine the range of effects of fracture pattern on rockfall, not to systematically cover all the possible fracture patterns at the repository.

Generation of fracture patterns included estimating a mean and a standard deviation from the mean for a uniform probability distribution for fracture spacing and orientation based on information provided for each primary fracture set (Pye et al. 1997). Individual judgment played an important role in selecting the mean and the standard deviation from the mean for the three fracture sets. Also, fracture trace length and persistence are mainly assumed. It should also be noted there are a number of limitations in the UDEC fracture generator: (i) it is limited to two dimensions (2D); (ii) fracture spacing, orientation, trace length, and persistence are assumed to have uniform distributions; and (iii) UDEC is not capable of handling fractures that do not completely intersect a block and therefore, many small fractures or segments of fractures are automatically deleted. These limitations make simulated fracture patterns different from *in situ* fracture patterns and, therefore, may affect stress distribution and failure of the rock mass. Further investigations are necessary to evaluate such effects. Ideally, a three-dimensional (3D) fracture generator that can account for a variety of distribution types should be used to generate fractures in 3D and obtain the required 2D cross section from the 3D model for mechanical analyses. Alternatively, fracture patterns on a typical cross section from the underground mapping data may be used to digitize the fractures and manually input them into the UDEC model. These options will be further explored in the future when more fracture data become available.

The current DOE thermal loading strategy uses the concept of areal mass load (AML in metric tons of uranium per acre, or MTU/acre). DOE thermal analyses show that 85 MTU/acre is the highest AML that will satisfy all the thermal goals (U.S. Department of Energy 1998). Therefore, for the current modeling study, 85 MTU/acre AML was used.

Considering the prescribed dimensions of the WPs to be disposed at YM, the DOE proposed six possible arrangements of WPs and calculated associated drift

Table 1. UDEC Version 3.0 parameters used to generate fracture patterns

Case	Fracture Set	Angle[1] Mean	Angle[1] Deviation[2]	Trace Length Mean	Trace Length Deviation[2]	Gap Length Mean	Gap Length Deviation[2]	Fracture Spacing Mean	Fracture Spacing Deviation[2]
A	1st	85	10	7.5	1	0	0	0.4	0.1
	2nd	20	5	5	1	0	0	0.75	0.1
B	1st	85	10	12	4	0	0.1	0.3	0.05
	2nd	20	8	6	2	0	0.1	0.75	0.4
	3rd	110	10	12	4	0	0.1	1.8	0.5
C	1st	85	10	7.5	1	0	0	0.4	0.1
	2nd	20	5	5	1	0	0	0.75	0.1
	3rd	110	10	12	4	0	0.1	1.8	0.5

[1] The angle is measured counter-clockwise from the horizontal axis. [2]Deviation is the standard deviation from the mean, assuming a uniform probability distribution.

and WP spacings (Table 2). These arrangements put a package containing vitrified HLW between every adjacent spent nuclear fuel (SNF) WPs. SNF WPs are either 21-pressurized water reactor (PWR), 44-boiling water reactor (BWR), or 12-PWR WPs. The DOE analysis shows that to maintain 85 MTU/acre AML, a uniform drift spacing of 28 m needs to be planned for the entire repository. For 28 m drift spacing, the WP spacing is calculated to be 13.26 m. The heat mass content [$Q(t)$] is the sum of a 44-BWR package [$Q(t)_{44BWR}$] and an HLW package [$Q(t)_{HLW}$](Table 2) for a single drift and one-unit cell width (U.S. Department of Energy, 1998):

$$Q(t) = Q(t)_{44BWR} + Q(t)_{HLW} \tag{1}$$

The average thermal decay for a 44-BWR package and an HLW package given in Table V-1 of DOE (1998) was used in calculating $Q(t)$. Assuming that heat is uniformly distributed on the drift wall, the decay heat flux $q(t)$ is calculated as

$$q(t) = \frac{Q(t)}{\pi D L_{wp}} \tag{2}$$

where D is drift diameter (5 m) and L_{wp} is center-to-center spacing between two adjacent SNF WPs (13.26 m). UDEC currently allows a thermal flux boundary condition to be input as a simple, exponentially decaying flux with a single decay coefficient of the form

$$q(t) = q_0 \exp(-\alpha t) \tag{3}$$

where q_0 is flux applied to the drift wall at time of emplacement and α is the decay constant (1/s). The initial heat flux was estimated to be 43.18 W/m^2. Eight decay segments of the form of equation 3 were obtained by a best-fit approach to approximate $q(t)$. Heat transfer by radiation or convection from the WP to the drift wall was neglected from these calculations, which may underestimate heat load. Also, heat removal from ventilation was neglected, which may overestimate head load.

TM properties (Table 3) were selected from a specific case of a previous study (case 12 of Ahola et al. 1996). This combination of intact and fracture TM properties caused relatively significant yielding and large shear displacement along fractures. These parameter values represent upper bounds on intact rock cohesion and intact rock Young's modulus; lower bounds on fracture friction angle, thermal expansion coefficient, and intact rock friction angle; and averages for the other parameters. The upper and lower bound and average values were selected based on information available from a number of DOE sources as detailed in Ahola et al. (1996).

Since the main purpose of the current study is to establish an approach to explicitly model rockfall, seismic ground motion input was kept simple. A simple sigmoidal dynamic signal was used, with a maximum peak ground acceleration of approximately 0.4 g and frequency of 10 Hz. Potential effects of various characteristics of a more realistic earthquake time history will be investigated in the future. The dynamic signal was applied to the base of the model as a vertically propagating compressive stress wave.

2.2 *Model geometry and boundary conditions*

Selections of the geometric model and boundary conditions were based on the assumption of multiple parallel drifts. The study simulated a single drift placed in the middle of a group of similar drifts parallel to each other. The drifts were assumed to be long enough so that plane-strain condition applies. All fractures were assumed 2D and had strikes parallel to the drift. Drift diameter was 5 m and drift spacing 28 m.

Figure 1 depicts the geometric model comprised of discrete element blocks for case C. The model extended vertically from ground surface (about 317 m above the repository) to approximately groundwater level (about 350 m below the repository). At such extent, heat flux due to emplaced WPs is almost zero and the ambient temperatures applied along the upper and lower boundaries do not influence the results in the area around the drift for the selected simulation time of 100 yr in the case with thermal loading. To maintain a reasonable and workable problem size, only a region approximately one drift diameter in the rock mass was modeled as having the specified fracture spacings.

Table 2. Six possible spent nuclear fuel waste package combinations and associated drift and waste package spacings (U.S. Department of Energy 1998)

	Waste Package	Maximum Drift Spacing, m	Waste Package Spacing, m
1	21-PWR HLW 44-BWR	30	13.28
2	21-PWR HLW 21-PWR	32	13.3
3	21-PWR HLW 12-PWR	25	13.67
4	44-BWR HLW 44-BWR	28	13.26
5	44-BWR HLW 12-PWR	23	13.68
6	21-PWR HLW 12-PWR	19	13.58

Table 3. Intact rock and fracture thermal-mechanical properties (Ahola et al. 1996)

Parameters	Parameter Values	Unit
Young's Modulus	32	GPa
Poisson's Ratio	0.21	—
Rock Friction Angle	20	degrees
Rock Cohesion	43	MPa
Rock Tensile Strength	5	MPa
Rock Compressive Strength	166	MPa
Rock Density	2297	kg/m^3
Fracture Friction Angle	38	degrees
Fracture Cohesion	0.08	MPa
Fracture Tensile Strength	0.04	MPa
Fracture Normal and Shear Stiffness	1.0×10^{-5}	MPa/m
Fracture Angle of Friction	0.04	—
Thermal Expansion Coefficient	6×10^{-6}	K^{-1}
Thermal Conductivity	2.1	W/m-K
Specific Heat	932	J/Kg-K

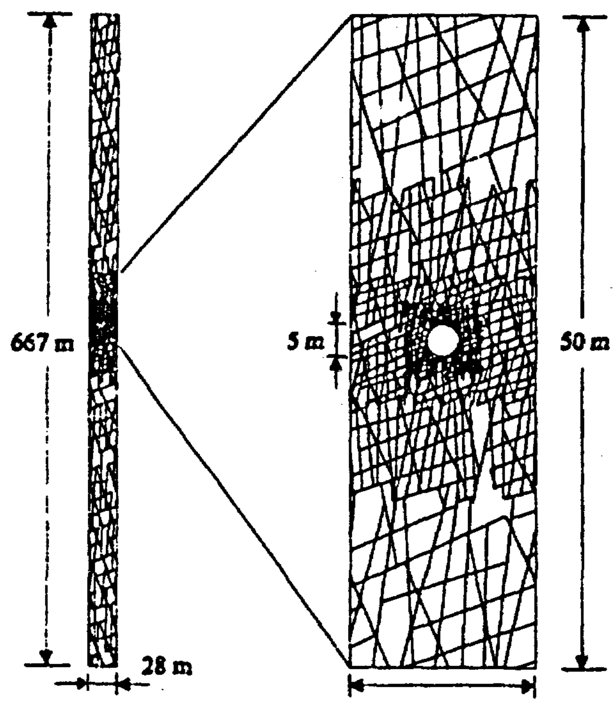

Figure 1. Model geometry showing blocks and a particular fracture pattern (case C). (a) full model for TM analyses. (b) Submodel for dynamic analyses.

Beyond this region, block size was gradually scaled up, whereas a comparable fracture pattern was maintained. Zoning was also scaled accordingly. Ground support of the drift was not modeled.

The vertical boundaries represented lines of symmetry based on the assumption of multiple parallel drifts and were assigned zero horizontal displacement and heat flux. The top boundary representing the ground surface was stress free and the bottom boundary was fixed in the vertical direction. Temperature was fixed at 18.7 °C at the top boundary and 34.2 °C at the bottom boundary. The *in situ* vertical stress at the repository horizon was set to be 7.0 MPa based on average measured values in the DOE advanced conceptual design (Civilian Radioactive Waste Management System, Management and Operating Contractor 1996). The vertical stress gradient with depth was 0.0221 MPa/m based on rock density. The *in situ* horizontal stress was assumed related to the vertical stress by Poisson's ratio. This assumption gives a stress ratio that is within the range of stress ratios measured at YM (Harmsen 1994, Stock et al. 1985).

For dynamic analyses, a smaller submodel of the original domain was used to reduce the size of the problem and computational time. This was achieved after the initial TM analyses. Solutions of stresses, temperature, and displacements from the TM analyses were used as the initial conditions for the subsequent dynamic analyses. The submodel extended 50 m above and below the repository horizon (Fig. 1). For this preliminary study, only a vertically propagating compressive wave was applied. Therefore, the vertical boundaries remained rollered. After solving for the new boundary stresses (from the solution of the TM modeling) to be applied to the upper and lower boundaries of the submodel, viscous nonreflecting boundary conditions were also applied to these boundaries. For the base of the model, this required simulating the earthquake signal as a stress-time rather than velocity-time history using UDEC.

2:3 *Modeling approach*

The simulation started by obtaining an initial model equilibrium under *in situ* stress and excavating the tunnel. After these initial analyses, the mechanical time was reset to zero for the TM analysis. UDEC uses a sequential coupling approach in conducting a TM analyses. This approach consists of running the thermal analysis for a period of time during which the nodal or grid-point temperatures are updated. The thermal time is then held fixed while mechanical cycling is conducted to update stresses, displacements, and block rotations to reach a new mechanical equilibrium. In such analyses, thermal time is the actual simulation time whereas the mechanical time is a pseudo-time for the intermediate calculations. An implicit thermal solution scheme was chosen to allow the user to specify a thermal time step.

For each fracture pattern listed in Table 1, two analyses were performed. The first (cases A, B, and C) assumed no thermal load and were subjected to only *in situ* stress and dynamic load. For the second set of analyses (cases A1, B1, and C1), the time-decay thermal load was applied to the drift for 100 yr. At 100 yr, dynamic analysis was conducted. When desirable, the seismic load was repeated to examine the effect of repetitive seismic load on rockfall.

3 MODELING RESULTS

Modeling results discussed are explicit rockfall, fracture shear and normal displacements, yield of intact rock blocks, and the relationship among rockfall, fracture displacement, and yielding. The combination of these observations may provide indications of the maximum extent of the potential rockfall region. The observations may also be used as indices for establishing a rockfall criterion.

3.1 *Explicit rockfall*

Explicit rockfall after one episode of earthquake ground motion is shown for cases A (Fig. 2), B (Fig. 3), and C (Fig. 4). Rockfall in case A was limited to the upper-right corner of the drift. The drift appeared to be in a rather stable condition after the first rockfall because a second episode of earthquake ground motion did not induce further rockfall. Case C had the most extensive rockfall. Rock blocks within a wide region extending 3–3.5 m into the roof area fell into the drift simultaneously after one episode of seismic load, causing the entire opening to collapse. Comparison of the cross-sectional area of the opening with the area of the simulated rockfall region indicated that this particular rockfall event could fill most of the drift with falling blocks and completely bury the WP. The drift appeared unstable after the first episode of seismic load and rock blocks continued to fall. In case B, the upper-right corner and the first layer of blocks fell after the first episode of seismic load. The extension of the region of rockfall on the upper-right corner was much greater than for case A. Continuing analysis showed the upper-right corner was rather unstable, causing collapse of the drift wall on the right-hand side.

As indicated by fracture patterns shown in Figures 2-4 and fracture parameters shown in Table 1, the fracture pattern was the simplest in case A, which included two fracture sets. The first two fracture sets in case B were essentially the same as those in case A, except case B included a third fracture set oriented

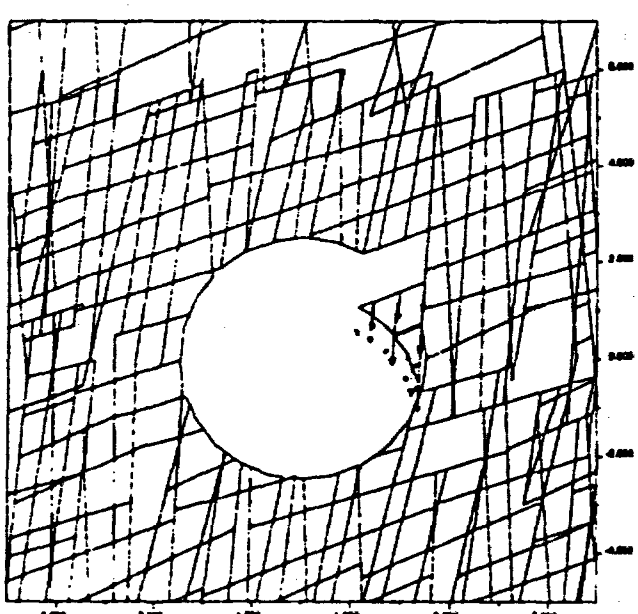

Figure 2. Explicit rockfall after one episode of earthquake ground motion for case A (unheated drift).

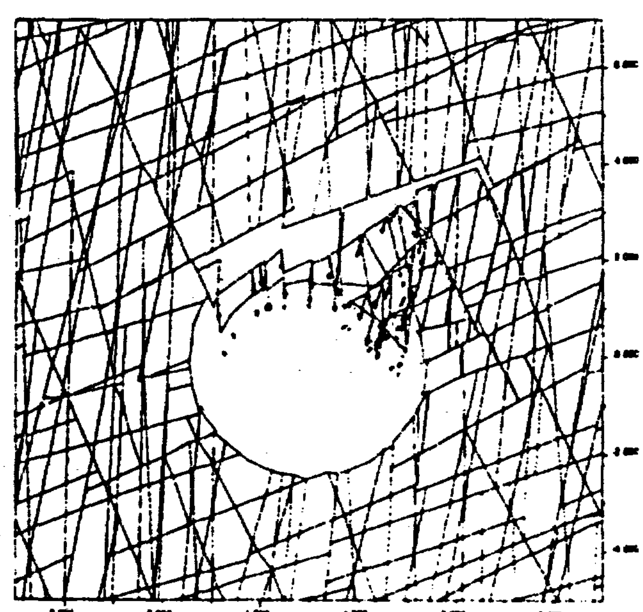

Figure 3. Explicit rockfall after one episode of earthquake ground motion for case B (unheated drift)

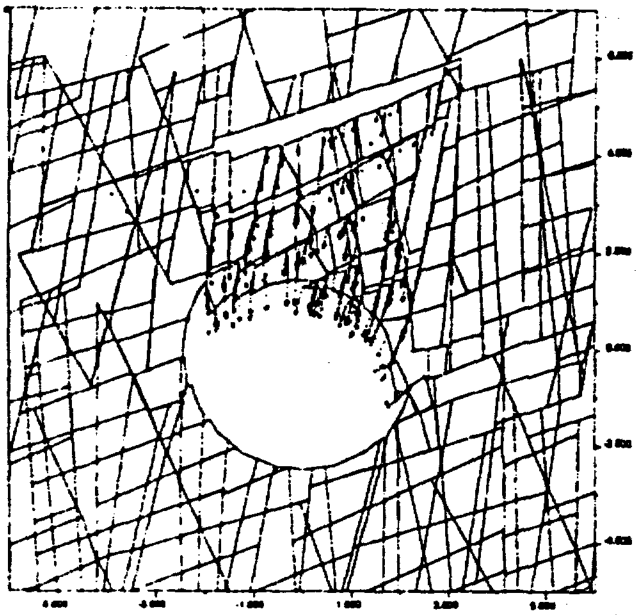

Figure 4. Explicit rockfall after one episode of earthquake ground motion for case C (unheated drift)

about 110° from the x-axis. Although this third fracture set had large spacings, its inclusion in the model increased the amount of simulated rockfall significantly. Fracture pattern in case C was similar to that in case B, however, block size was smaller and more irregular in the roof region. These comparisons indicate that the more irregular the fracture pattern, the more extensive the rockfall. Rockfall also depends on block size: the smaller the block size, the more extensive the rockfall.

In the case of heated drifts (i.e., conducting TM analyses for 100 yr prior to dynamic analyses), some rock blocks fell during the thermal loading stage. For example, the blocks on the upper-right corner in case A1 fell during the thermal loading and then the opening appeared stable with no further falling blocks during seismic load. In case B1, blocks on the upper-right corner loosened during thermal loading and eventually fell at the early stage of seismic loading. It is interesting to note that the region involving rockfall for the case of heated drift is actually smaller than that in the case of unheated drift. Repeated seismic load did not cause further rockfall. A similar phenomenon was also observed in case C1. Blocks in the roof region in case C1 loosened during thermal loading and gradually fell during the early stage of seismic loading. Similar to case B1, the region involving rockfall in the case of heated drift is somewhat smaller than that of an unheated drift during the first episode of seismic loading. This may be attributed to the upward thermal stress that counteracts the downward stress due to dynamic load in the roof region when the drift is under thermal load. Rockfall continued during the subsequent modeling and the opening appeared unstable.

3.2 *Fracture displacement*

Thermal loading has been observed to generally increase fracture shear and normal displacements (Ahola et al. 1996) around an unsurported drift under *in situ* stress. A similar phenomenon was observed in the current study. Furthermore, seismic load appears to increase both fracture shear displacement and fracture opening significantly. An increase in fracture displacement was observed in all three cases for both heated and unheated drifts. It is not practical, however, to quantify these changes in fracture displacements at the current stage. Further modeling effort is necessary.

3.3 *Yield of intact rock blocks*

Yield of intact rock blocks was observed previously to increase with thermal load (Ahola et al. 1996), and if extensive yield had already occurred during thermal loading, seismic load will further increase the yield (Ahola 1997). A similar phenomenon was also observed in the current study. Since the yield of intact rock depends largely on rock TM properties, conclusions with regard to the yield cannot be drawn at this stage. Future studies will consider the effect of fracture and intact rock TM properties.

4 DISCUSSION

As discussed earlier, fracture pattern appears to control the amount of simulated rockfall. With increasing complexity of fracture patterns, especially significantly varying orientations, and decreasing block sizes (or fracture spacings), it appears the number of rock blocks falling and the extent of a rockfall region increase. Irregularity of fracture pattern appears to be an essential condition for explicit rockfall, since earlier attempts to explicitly simulate rockfall failed when a regular fracture pattern was used (e.g., Ahola 1997). It is noted that even with the same set of fracture parameters (i.e., statistical data summarized based on field mapping and other measuring results), the generated fracture pattern could be slightly different. The slight difference in fracture pattern, especially near the roof area, could result in a different amount of rockfall during each seismic ground motion episode. The controlling effect of fracture patterns, particularly of irregular nature, on underground opening stability has been observed in the literature (e.g., Bhasin & Hoeg 1998). Quantifying the effect of fracture pattern on rockfall for the purpose of repository performance assessment is a challenging and on-going process. It is important to characterize fracture distribution and generate fracture patterns representative of the *in situ* fracture pattern at the repository. The fracture generator in UDEC is limited to a uniform distribution. As mentioned previously, most fracture parameters (e.g., fracture spacing and inclination angle) show a log-normal distribution at YM. Also, controlling the generated intact block size in the current version of UDEC is achieved by adjusting the fracture spacing, which also alter fracture pattern and is not straightforward. Additional external calculations are necessary to estimate the generated block size distribution. Therefore, it is not easy to isolate the effect of block size with similar fracture patterns on rockfall. These modeling difficulties need to be resolved before attempts can be made to quantify the effect of fracture pattern and block size on rockfall.

Fracture patterns may have significant spatial variations within the repository, depending on the nearby stratigraphic and faulting characteristics. It is, therefore, necessary in future studies to consider an array of fracture patterns. To accomplish this, review of the results of a detailed study of fractures is necessary. Two approaches have been considered: (i) using a more applicable fracture generator and generate fracture patterns based on statistical fracture parameter data from detailed fracture studies and (ii) digitizing selected fracture mapping results, such as the full-periphery mapping at the ESF main drift with tunnel curvature corrected. The second approach is rather straightforward and relatively easy to interpret. The representiveness of the selected sections, however, may be limited, and quantification of the fracture pattern using statistical distribution data may need additional analyses of the digitized fracture profile. The first approach should be more representative statistically; however, it requires significant effort in identifying and using a practical fracture generator and detailed fracture study.

Another important aspect of the *in situ* fracture geometric characteristic is block size distribution. *In situ* block size distribution is also important in assessing the potential effect of rockfalls on WPs—it provides a lower bound for the potential impact force on the WPs by falling blocks. Some research has been done on *in situ* block size at YM. For example, Gauthier et al. (1995) estimated size distribution of individual rock blocks using a modified (log-space) version of the Topopah Spring fracture spacing distribution developed by Schenker et al. (1995), assuming cubic and parallelpiped blocks. It should be noted that assumptions of cubic or parallelpiped block shape may distort the estimation of size distribution of *in situ* blocks through various assumptions with regard to the extent of fractures in 3D. In published literature in recent years, several models have been developed capable of simulating the 3D nature of a rock mass (e.g., Dershowitz & Einstein 1988). These models differ in degree of complexity and sophistication, as well as basic theoretical background (e.g., finite/infinite fracture size and block shape). Examples include the Simblock model developed by Peaker (1990), the Blocks model developed by Maerz & Germain (1992), and the Stereoblock model developed by Hadjigeorgiou & Grenon (1998). These models will be further examined and applied to analyzing block size distributions at YM.

As indicated in section 2.1, seismic ground motion input in the current modeling study was a sigmoidal dynamic signal to simplify the problem. Preliminary analyses with different frequency content (1 to 10 Hz) show little effect on qualitative rockfall. In an actual earthquake time history, the acceleration pulses are of varying amplitudes and frequencies. Since ground motion at a particular site is influenced by source, travel path characteristics, and local site conditions, it may be important in dynamic response analyses to use ground motion input that is site specific. However, the current study indicates that fracture pattern and block size may have much greater effect on rockfall than the input seismic time history. The amplitudes of ground motion are expected to have a significant effect on rockfall. Currently used amplitude represents a higher bound design earthquake amplitude at the repository interface (Risk Engineering, Inc. 1998).

It is recognized that current information and the level of understanding regarding long-term degradation of the rock mass within the near-field repository environment is limited. As a result, the previous parametric study of stability of drift under static load employed ranges of TM parameters measured in the laboratory or field to account for the variation of parameters at the YM site as well as how they may change or degrade with temperature, time, stress, and moisture content (Ahola et al. 1996). The effect of rock and fracture TM properties on stability of drift under dynamic load will be considered and studied in more detail in the future. Again, it is anticipated that the effect of rock and fracture TM properties on rockfall due to dynamic load may be much less significant compared to the effect of fracture patterns and block size.

For block dynamic analysis of a discontinuum system, several factors may affect modeling results significantly and such effects need to be understood in future modeling exercises. These considerations may include mechanical damping, wave transmission in a discontinuum system, boundary conditions, and loading approach. Currently, the performance of the UDEC code with regard to how these factors may have affected modeling results is not yet well understood.

To quantify rockfall parameters, it is desirable to establish a rockfall criterion to define the vertical extent of the potential rockfall region using indices such as the amount of explicitly simulated rockfall, fracture shear and normal displacements, stress state and, consequently, yielding of intact rock blocks. Such a criterion would depend largely on fracture pattern and size of *in situ* rock blocks, and to a lesser degree, on earthquake ground motion and rock and fracture TM properties. Due to the importance of fracture pattern and block size in rockfall analyses, it may be very useful to conduct Key Block analyses prior to dynamic simulation for each generated fracture model and use certain indices of the Key Block Theory as indicators of rock mass stability.

5 CONCLUSION

Fracture pattern appears to have controlling effects on the amount of explicitly simulated rockfall. With increasing complexity of fracture patterns (especially significantly varying orientations and increasing irregularity), the number of rock blocks falling, the extent of the rockfall region, and the overall drift instability increase. Further research is necessary to quantify rockfall parameters for the purpose of repository performance assessment through better quantification of fracture pattern, block size, earthquake ground motion characteristics, and rock block and fracture TM properties.

ACKNOWLEDGMENT

The author would like to thank Drs. W.C. Patrick and S.M. Hsiung for their insightful review of the paper. The work was performed by the Center for Nuclear Waste Regulatory Analyses (CNWRA) for the Nuclear Regulatory Commission (NRC) under contract number NRC-02-97-009. The report is an independent product of the CNWRA and does not necessarily reflect the views or regulatory position of the NRC.

REFERENCES

Ahola, M.P., R. Chen, H. Karimi, S.M. Hsiung & A.H. Chowdhury 1996. *A Parametric Study of Drift Stability in Jointed Rock Mass, Phase I: Discrete Element Thermal-Mechanical Analysis of Unbackfilled Drifts.* CNWRA 96-009. San Antonio, TX.

Ahola, M.P. 1997. *A Parametric Study of Drift Stability in Jointed Rock Mass—Phase II: Discrete Element Dynamic Analysis of Unbackfilled Drifts.* CNWRA 97-007. San Antonio, TX.

Anna, L.O. 1998. *Preliminary Three-Dimensional Discrete Fracture Model of Topopah Spring Tuff in the Exploratory Studies Facility, Yucca Mountain Area, Nye County, Nevada.* USGS Open-File Report 97-834.

Beason, S.C. 1997. Previous mapping efforts. *Handout and presentation at U.S. Department of Energy/Nuclear Regulatory Commission Appendix 7 Meetings, October 16, 1997.* Washington, DC.

Bhasin, R. & K. Hoeg 1998. Parametric study for a large cavern in jointed rock using a distinct element model (UDEC-BB). *Int. J. Rock Mech. Mining Sci.* 35(1): 17–29.

Brechtel, C.E., M. Lin, E. Martin & D. S. Kessel 1995. *Geotechnical Characterization of the North Ramp of the Exploratory Studies Facility.* SAND95–0488/1. Albuquerque, NM.

Civilian Radioactive Waste Management System, Management and Operating Contractor 1996. *Mined Geologic Disposal System Advanced Conceptual Design Report.* Volume II. B00000000–0717–5705–00015. Rev. 0. Las Vegas, NV.

Dershowitz, W.S. & H.H. Einstein 1988. Characterizing rock joint geometry with joint system models. *Rock Mech.* 21: 21–51.

Gauthier, J.H., M.L. Wilson, D.J. Borns & B.W. Arnold 1995. Impacts of seismic activity on long-term repository performance at Yucca Mountain. *Focus '95: Proceedings of the Methods of Seismic Hazards Evaluation.* La Grange Park, IL: 159–168.

Hadjigeorgiou, J. & M. Grenon 1998. Defining in-situ block size. *Can. Mining Metal. Bull.* 91(1020): 72–75.

Harmsen, S.C. 1994. The Little Skull Mountain, Nevada, earthquake of 29 June 1992: aftershock focal mechanisms and tectonic stress field implications. *Bull. Seismol. Soc. Am.* 84 (5): 1484-1505.

Itasca Consulting Group, Inc. 1996. *UDEC—Universal Distinct Element Code. Version 3.0, Volume I: User's Manual.* Minneapolis, MN.

Lin, M., M.P. Hardy & S.J. Bauer 1993. *Fracture Analysis and Rock Quality Designation Estimation for the Yucca Mountain Site Characterization Project.* SAND92–0449. Albuquerque, NM.

Maerz, N.H. & P. Germain 1992. Block size determination around underground openings using simulations based on scanline mapping. *Preprints of the International Society for Rock Mechanics Conference on Fractured and Jointed Rock Masses, Lake Tahoe, Nevada.* Berkeley, CA.

Peaker, S.M. 1990. *Development of a simple block size distribution model for the classification of rock masses.* Master's thesis, University of Toronto.

Pye, J.H., D.C. Kicker & G.H. Nieder-Westermann 1997. Plans for mapping of subsurface Facilities. *Notes from U.S. Department of Energy/Nuclear Regulatory Commission Appendix 7 Discussions.* October 16, 1997.

Risk Engineering, Inc. 1998. *Seismic Design Basis Inputs for a High-Level Waste Repository at Yucca Mountain, Nevada.* B00000000-01727-5700-0018, Rev. 0.

Schenker, A.R., D.C. Guerin, T.H. Robey, C.A. Rautman & R.W. Barnard 1995. *Stochastic Hydrogeologic Units and Hydrogeologic Properties Development for Total-System Performance Assessments.* SAND94–0244. Albuquerque, NM.

Stock, J.M., J.H. Healy, S.H. Hickman & M.D. Zoback 1985. Hydraulic fracturing stress measurements at Yucca Mountain, Nevada and relationship to regional stress field. J. Geophys. Res. 90 (B10): 8691-8706.

U.S. Department of Energy 1998. *Repository Thermal Loading Management Analysis.* B00000000–01717–0200–00135. Rev. 0.

Wernicke, B.P. 1992. Cenozoic extensional tectonics of the Western Cordillera. The Cordilleran Orogen: Conterminous U.S. B.C. Burchfiel, P.W. Lipman and M.C. Zoback (eds), *The Geology of North America.* Boulder, CO: Geological Society of America G-3: 553–581.

Wong, I.G. & J.C. Stepp 1998. *Probabilistic Seismic Hazard Analyses for Fault Displacement and Vibratory Ground Motion at Yucca Mountain, Nevada.* Final report. Oakland, CA.